Spectral Characterization of Shoemaker Crater at the lunar south pole: Possible science objective for the Artemis III Human Mission to Moon

Prateek Tripathi (1), Rahul Dev Garg (1)

[1] Geomatics Engineering Group, Department of Civil Engineering,
Indian Institute of Technology, Roorkee, Uttarakhand, India, 247667
Email: ptripathi@ce.iitr.ac.in; rdgarg@ce.iitr.ac.in

KEY WORDS: Moon, Hyperspectral Remote Sensing, Mineralogy, Spectral Characterization, Feature Detection

ABSTRACT: The upcoming Artemis mission of NASA is planned to land humans within 6 degrees of the lunar South Pole. This work analyzes spectral parameters obtained from hyperspectral datasets to characterize the Shoemaker crater in the lunar south pole region as one of the landing sites for the Artemis III mission. This work utilizes the hyperspectral data from Moon Mineralogy Mapper of Chandrayaan-1 launched by the Indian Space Research Organisation, to extract the band depth, slope, band center, and band area. There is a possibility of cold water traps in this crater as it is one of the permanently shadowed areas and falls within 6 degrees of the south pole. Comparison of spectral parameters from shoemaker crater and Hutton impact crater (far side) and Le Verrier, a lunar impact crater on the north of the Mare Imbrium (near side), shows the difference in band parameters at 2000nm. The band depth and band slope trends, Integrated Band depth indices, and Optical maturity parameters are also showing significant differences. The spectral trends also depict that these regions have reflected the solar wind ions and depositions of various ions due to cometary impact; hence they can provide much important science about lunar swirls or magnetism. The extraction of hydrogen from the bottom of the craters in the lunar south pole and its analysis for solar wind ion and the cometary impact can be one of the Artemis III mission's science objectives.

1. INTRODUCTION

NASA is planning to launch the Artemis III mission by 2024 to the lunar south pole, which is also called as the first human mission in the 21st century with a crew of two, to the surface of the Moon. The science activities are also being finalized. The landing site will be finalized later but will be within 6 degrees of the South pole. The landing site should be suitable for a two-member crew to collect lunar samples, deployment of cameras, sensors, and other portable instruments, and multiple walking excursions to be done for scientific experiments (NASA, 2020). This work discusses the comparative spectral analysis of Shoemaker crater (88° 6′ S, 44° 54′ E) with the caters on the far and near side of the Moon. The motive of this work is to suggest the Shoemaker crater as one of the potential landing sites for Artemis III.

Although the vicinity of the previous landing site of Apollo missions could be a better option for the landing of Artemis III as the crew will not need to start from zero as they already have enough information from the returned samples. However, recent research has developed a ray of hope among researchers that water ice on lunar poles can be vital for crewed missions. This work majorly pints towards this fact only.

Shoemaker crater, which comes into notice after the Lunar Prospector mission in 1999 crashed into the crater in a failed attempt to detect water ice by generating vapor due to impact. However, few permanently shadowed regions have been there on the lunar poles, in the dark for many years, and there will be the possibility that they may contain water ice deposited by the bombardment of comets and water-bearing asteroids (ESA, 2014). One of the efficient ways to detect the water ice

is by analyzing hyperspectral datasets of the lunar surface for mineralogy and maturity.
The results from the analysis of hyperspectral datasets of the lunar south pole near to dark areas can provide the new insights about moon's history and the interaction process of the Moon with the Earth over its history.

2. MATERIALS AND METHODS

The hyperspectral data from Moon Mineralogy Mapper (M^3) onboard Chandrayaan-1 mission of ISRO is used to analyze the spectral and mineralogical properties of the Lunar surface. The satellite data is downloaded from the Lunar Orbital Data Explorer (https://ode.rsl.wustl.edu/). It has the following specifications: spatial resolution of 140 m/pixel globally and doubled from 200km orbit, spectral coverage of 446-3000nm (86 bands) with a swath of 40km. It has a spectral resolution in the range of 20-40nm. The M^3 data is captured in two optical periods, defined by favorable viewing conditions. The M^3 technical team subdivided the optical periods based on data characteristics. The M^3 data utilized in this work is from the optical period 1B (Carle M Pieters et al., 2009). Due to thermal noise and spectral reddening of the slope after 2500nm, only 72 bands (500-2500nm) are considered in this work. Band 1 and Band 2 have no data hence discarded. Data from different optical seasons are avoided due to differences in detector temperature, resulting in a difference in reflectance. However, in the case of no data, different periods are considered.
The spectral analysis is carried out for three locations, one each at south pole, Mare and Highlands region, i.e., Shoemaker lunar impact crater (88° 6′ S, 44° 54′ E) lies within half a crater diameter of Shackleton at the lunar south pole (Figure 1a), second is Helicon (40° 24′ N, 23° 6′ W) and Le Verrier (40° 18′ N, 20° 36′ W) impact craters (Figure 2a) located in the northern part of the Mare Imbrium, and the third is Hutton impact crater with other nearby craters (37° 18′ N, 168° 42′ E), on the far side of the Moon (Figure 3a).
The satellite data is georeferenced and mosaicked using ENVI software. The vertical normalized spectral profile from various key locations from the selected study area have been analyzed for lithological composition and band parameters, including band center, depth, and slope (Figure 5). Savitzky Golay smoothing technique is used to smoothen the continuum removed spectra with interval 11 and polynomial order 3 (Press & Teukolsky, 1990; Savitzky & Golay, 1964). A very large number of sampling intervals in the Savitzky-Golay technique can suppress the important spectral features by over-smoothening. The 1000nm and 2000nm absorption band location is observed (Figure 1, Figure 2, and Figure 3). These spectra are extracted in a straight downward direction (vertical profile) at each location, considering space weathering, as marked. IBD and OMAT parameters were also calculated.

2.1 Integrated Band Depth (IBD)

IBD can calculated using the equation below (1):

$$\text{IBD at 1 } \mu\text{m} = \sum_{n=0}^{26} 1 - \left(\frac{R(789+20n)}{R_c(789+20n)}\right)$$

$$\text{IBD at 2 } \mu\text{m} = \sum_{n=0}^{26} 1 - \left(\frac{R(1658+40n)}{R_c(1658+40n)}\right) \quad (1)$$

Where R is the reflectance at a particular wavelength, and R_c is the continuum removed reflectance. IBD will help provide the fundamental mineralogical properties of the Lunar surface by representing the area which is having mafic silicates, showing soil maturity and space weathering (Figure 1b, Figure 2b, and Figure 3b). IBD can summarize the mineral diversity of the lunar surface with M^3 data (Mustard et al., 2011).

2.2 Optical Maturity (OMAT)

This parameter is used for checking the effect of space weathering on the lunar surface (soil). Space weathering represents the physical process, which tells how much the lunar surface is affected by the bombardment of solar wind ions and other cosmic rays resulting in the change of the optical properties. The optical maturity parameter is calculated using the formula given in equation (2):

$$\text{OMAT}= \sqrt{(R_{750} - R_0)^2 + (\left(\frac{R_{950}}{R_{750}}\right) - R_1)^2} \quad (2)$$

Where R_{750} is the reflectance at 750nm of a pixel or spectrum, and R_{950} is the reflectance at 950nm of a pixel or spectrum (Figure 2c and Figure 3c). The constants R_0 and R_1 apply to Clementine data only and must be used with the Clementine datasets (Baronia & Sarup, 2019; Lucey, Taylor, & Hawke, 1998; Nettles et al., 2011). Constants for M^3 datasets of the Apollo 17 landing site have been obtained by plotting the graph between R_{950}/R_{750} and R_{750}, i.e., 0.04,1.08.

3. RESULTS AND DISCUSSIONS

IBD (Integrated Band Depth) maps show the possible olivine-bearing /high mafic minerals in green-yellow color and the blue color for anorthosite or weathered minerals at Highlands. However, in Figure 1b, the yellow color showing the shadowed region on the south pole. This should not be confused with mafic minerals, as seen in the other two regions. The IBD shows the presence of anorthosite as the only mineral found near Shoemaker crater or in the vicinity of the south pole. In Figure 2b, the Helicon and Le Verrier craters have mafic minerals as there composition while the remaining areas are anorthosite. For study area 3, in Figure 3b, the anorthosites are present near Hutton and Trumpler crater while other areas have mafic minerals. The maps are also showing iron abundance around the Mare and Highlands regions. 1500nm band is chosen as a blue band because it has no specific absorption, as observed in M^3 data. These IBD maps infer the compositional differences at Mare and Highlands regions.

OMAT, on the other hand, represents the bright surface as young, also called immature, while dark as matured with low albedo values (Grier et al., 2001; Lucey et al.,2000; Lucey et al., 1998). However, there are striping issues in OMAT but the area in the vicinity of Helicon and Le Verrier, seen matured as compared to the surrounding (Figure 2c). For study area 3, the Hutton crater is only a mature body compared with the surroundings (Figure 3c).

The continuum removed smoothened spectra of M^3 observes two major spectral features at 1000nm and 2000nm, showing olivine and pyroxene for both study areas (Figure 1, Figure 2, and Figure 3). The shift observed in 1000nm and 2000nm dips are due to different space weathering processes across the lunar surface, but the weathering process is not efficiently described by the reflectance spectra alone (Bruck Syal & Schultz, 2015). Another reason may be the contribution of Mg^{2+}/Fe^{2+} in the M1 and M2 crystallographic sites or band shifts towards longer wavelengths due to Ca^{2+} (Adams et al., 1974; Pieters et al., 2019).

For study area 1, Shoemaker Crater, all locations have both diagnostic absorption features with band two at 1500nm instead of 2000nm. This makes this crater as an exciting region to explore by crewed missions. There is also a weak absorption band at 2000nm in locations 2 and 3, as seen in Figure 1b and Figure 1c. The shift observed in the 1000nm band for all locations, which may result from meteorite bombardment. For study area 2 in Figure 2(e, g, i), the diagnostic absorption features are 1000nm and 2000nm with a slight shift. For study area 3, in Figure 3 (e, g, and i), the 1000nm band is much more precise than 2000nm. The spectra are not much clear, but they exhibit diagnostic absorption features. This could be due to ferrous ion and also the Fe-Mg spinel exhibit a strong absorption feature near to 2000 nm with a slightly weaker feature at 1000 nm (Cloutis et

al., 2014). Plagioclase, belongs to feldspar group of minerals also shows absorption near 1250nm due to ferrous ion.

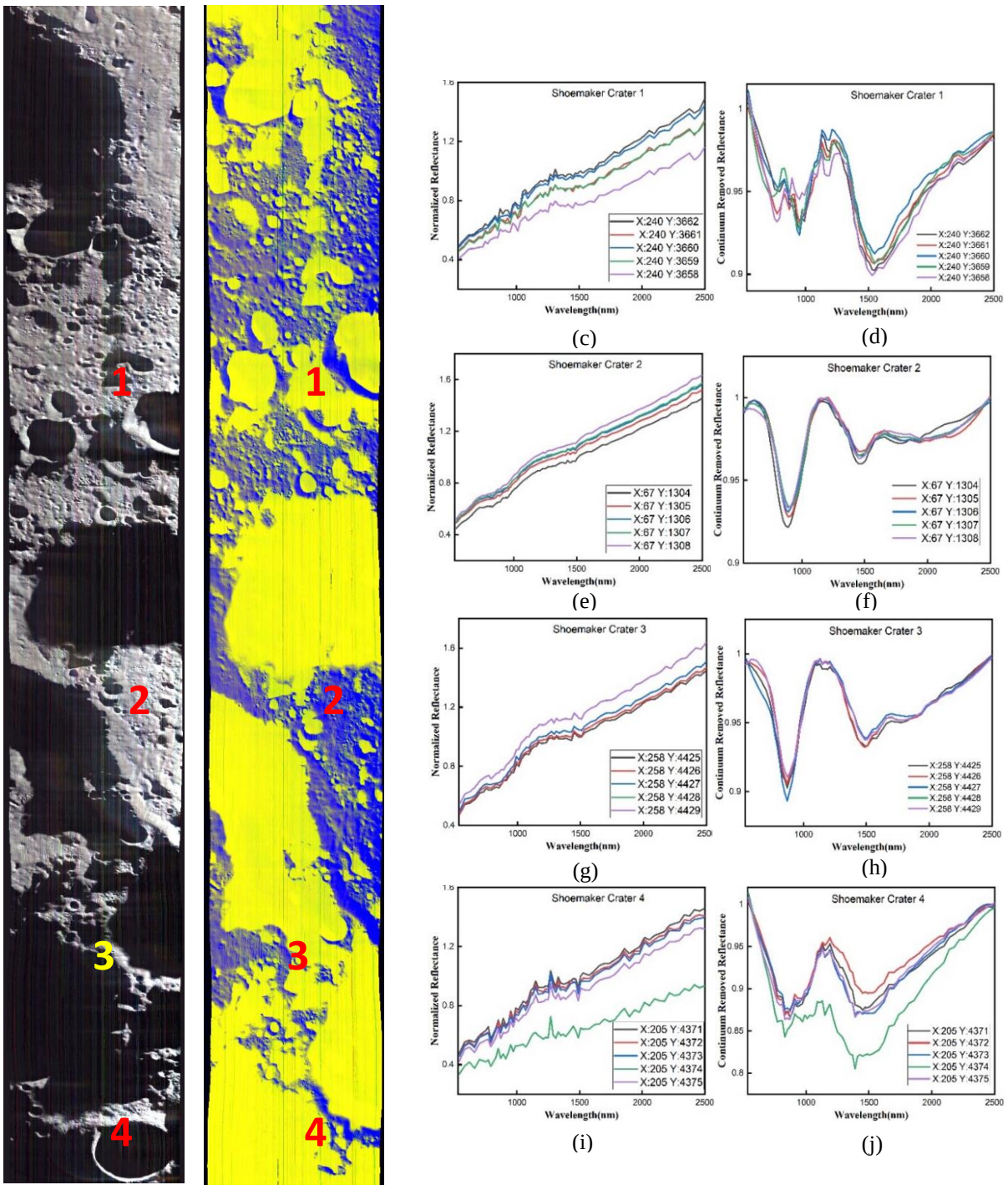

Figure 1 Shoemaker Crater at lunar south Pole (a) M^3 image with R= Band 14, G= Band 6, and B= Band 3. The location 1 is Highlands near Nobile Crater, location 2 is highlands near Shoemaker crater, location 3 is the rim of the Shoemaker Crater, and location 4 is the rim of Shackleton crater (b) Integrated Band depth image for Shoemaker crater. Here the yellow color depicts shadow while blue shows the anorthosite. Vertical Spectral profile for all the four regions as marked in (a) is shown in (c), (d), (e), (f), (g, (h), (i) and (j).

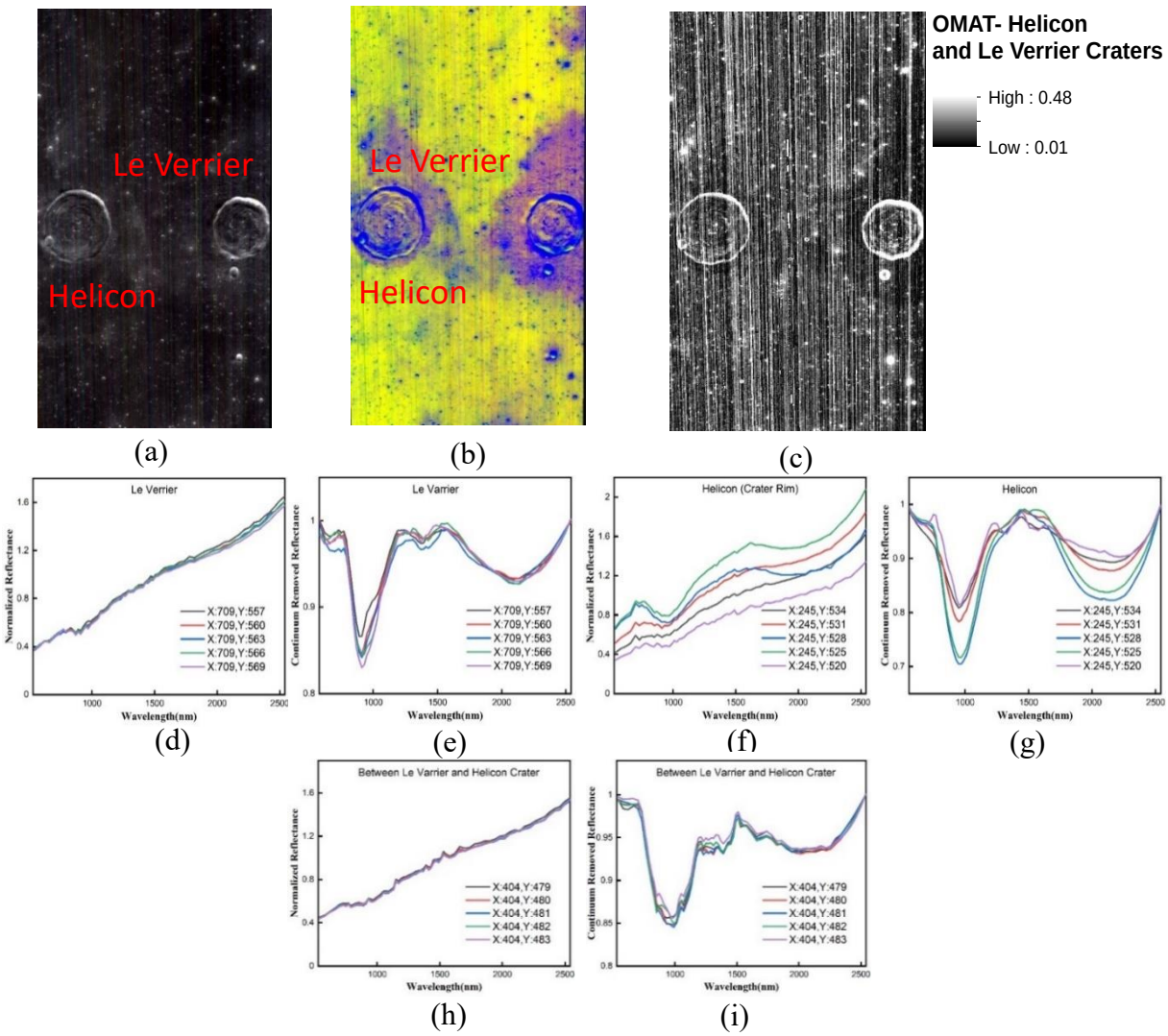

Figure 2 Helicon and Le Verrier Craters at lunar nearside (a) M^3 image with R= Band 14, G= Band 6, and B= Band 3 (b) Integrated Band depth image for Helicon and Le Verrier Craters. Here the yellow and blue color depicts the presence of mafic minerals and anorthosite, respectively. (c) Optical maturity (OMAT) parameter. The vertical spectral profile for both the craters and between them as marked in (a) is shown in (d), (e), (f), (g, (h), and (i).

For the calculation of Band Parameters, including band center, band depth, and band slope, third order polynomial fitting is used for spectra from all study areas (McCraig et al., 2017), including spectra extracted from Apollo 16 samples (Taylor et al., 2001). Apollo 16 is specifically chosen because of its location in south-central lunar Highlands. The Apollo 16 was landed about 50 kilometers to the north of the Descartes crater (11° 42′ S, 15° 42′ E).

The band center 1 (1000nm) vs. band center 2 (2000nm) graph for Shoemaker, Apollo, Hutton, and Helicon craters, illustrates the compositional trends of pyroxenes on the lunar surface (Figure 5a). Low and High calcium pyroxenes exhibit band centers which shift to longer wavelengths with increasing calcium and iron content (Low Ca), for High Ca pyroxenes, only the 1000nm band shifts to a longer wavelength. On the other hand, Mg-rich pyroxenes exhibit shorter wavelength band centers. Temperature also affects the absorption bands' position. As temperature rises, the 2000nm band shifts to shorter wavelengths for clinopyroxene and towards longer wavelengths for orthopyroxenes. The cooling history is also responsible for the shift in the 1000nm band position (Adams, 1974; Cloutis & Gaffey, 1991, 1993; Gaffey & Cloutis, 1991; Klima et al., 2011; Singer & Roush, 1985).

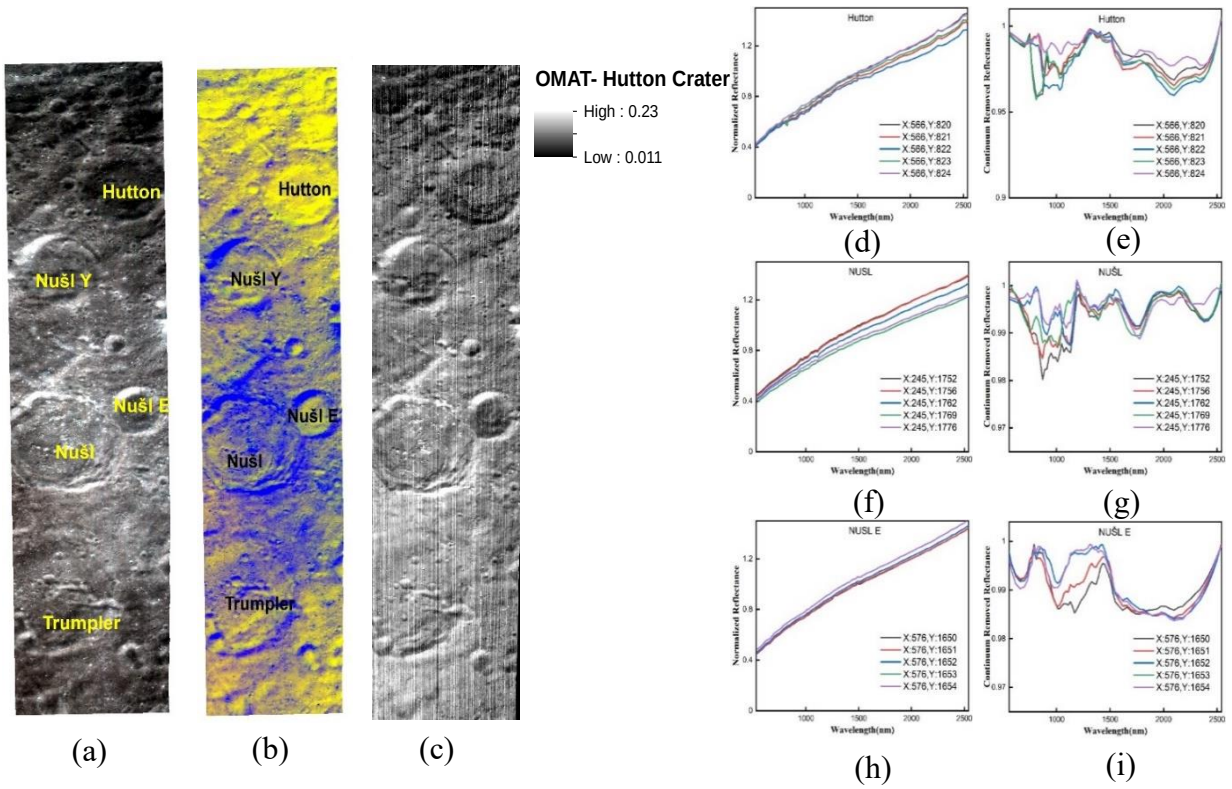

Figure 3 Hutton and nearby craters at the lunar far side (a) M^3 image with R= Band 14, G= Band 6, and B= Band 3 (b) Integrated Band depth image for Hutton. Here the yellow and blue color depicts the presence of mafic minerals and anorthosite, respectively. (c) Optical maturity (OMAT) parameter. The vertical spectral profile for both the craters and between them as marked in (a) is shown in (d), (e), (f), (g, (h), and (i).

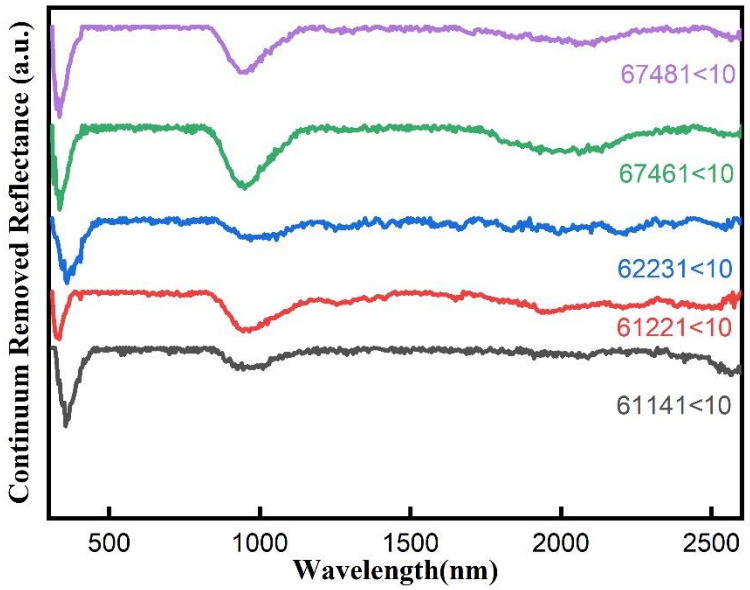

Figure 4 VNIR-SWIR Reflectance Spectra of samples returned from Apollo 16 Mission

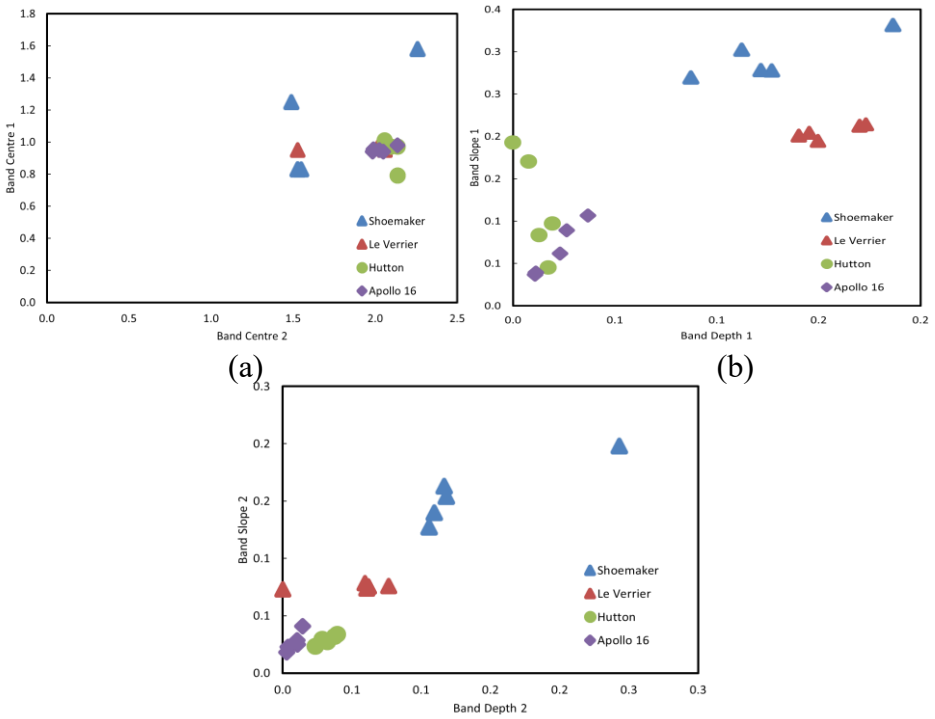

Figure 5 Band Parameters for all three study areas (a) Band center 1 at 1000nm vs. Band center 2 at 2000nm (b) Band Depth 1 at 1000nm vs. Band slope 1 at 1000nm (c) Band depth 2 at 2000nm vs. Band slope 2 at 2000nm

The trend of band centers also separates the shoemaker crater from Hutton crater and Apollo 16. Apollo 16 (near Descartes) and Hutton crater showing the same pyroxene compositions. However, the trends from band centers and Band depth vs. band slope graphs showing unexpected proximity for the Helicon, Le Verrier, and Shoemaker Craters. The band centers also sometimes refer to the complete pyroxene composition during exposure (Moriarty & Pieters, 2016). Band depths are positively correlated with Band slopes in Figure 5 (b, c). These trends represent space weathering effects—band Depths Vs. Band Slopes trends separate the Mare and Highlands regions (Nettles et al., 2010, 2011). For the shoemaker crater, larger the depth, higher the slope.

4. CONCLUSION AND FUTURE WORK

Initial trends from spectral analysis and band parameters show that Shoemaker Crater has its own unique properties, including the band center at 1500nm and being at extreme highlands but few similar properties with that of craters at Mare. The space weathering effect on optical properties was also seems similar to Apollo 16 samples collected near Descartes Crater. However, the increase in band depth with an increase in slope refers to broad and robust absorption features with pyroxene abundance and minimal space weathering effects.

The M^3 datasets gave limited details for this crater at the south pole because of few permanently shadowed regions (PSRs). One of the possible reasons is the striping error in datasets or calibration issues. Data from SAR (synthetic aperture Radar) will be integrated to explore the possibility of landing mission near PSRs. Also there are few contradicting spectral properties found during comparative spectral analysis of all study areas including the trends of band centers of mare and highlands region, makes the shoemaker crater an exciting site to explore. Based on spectral properties, it can be suggested that, during Artemis III, a crewed mission, it will be a good opportunity for the 2-member crew to do scientific experiments near the shoemaker crater and explore the hidden mystery of the lunar south pole.

5. REFERENCES

Adams, J. B. (1974). Visible and near-infrared diffuse reflectance spectra of pyroxenes as applied to remote sensing of solid objects in the solar system. Journal of Geophysical Research, 79(32),pp. 4829–4836.

Adams, J. B., Pieters, C., & McCord, T. B. (1974). Orange glass-Evidence for regional deposits of pyroclastic origin on the Moon. Lunar and Planetary Science Conference Proceedings, 5, pp. 171–186.

Baronia, A., & Sarup, J. (2019). Optical maturity on different crater using chandrayaan-1 M3 data. International Journal of Scientific and Technology Research, 8(12), pp. 2474–2477.

Bruck Syal, M., & Schultz, P. H. (2015). Cometary impact effects at the Moon: Implications for lunar swirl formation. Icarus, 257, pp. 194–206.

ESA. (2014). ESA - A peppering of craters at the Moon's south pole. Retrieved October 10, 2020, from http://www.esa.int/ESA_Multimedia/Images/2014/05/A_peppering_of_craters_at_the_Moon_s_south_pole

Grier, J. A., McEwen, A. S., Lucey, P. G., Milazzo, M., & Strom, R. G. (2001). Optical maturity of ejecta from large rayed lunar craters. Journal of Geophysical Research E: Planets, 106(E12), pp. 32847–32862.

Horgan, B. H. N., Cloutis, E. A., Mann, P., & Bell, J. F. (2014). Near-infrared spectra of ferrous mineral mixtures and methods for their identification in planetary surface spectra. Icarus, 234, pp. 132–154.

Klima, R. L., Dyar, M. D., & Pieters, C. M. (2011). Near-infrared spectra of clinopyroxenes: Effects of calcium content and crystal structure. Meteoritics & Planetary Science, 46(3), pp. 379–395.

Lucey, P. G., Blewett, D. T., Taylor, G. J., & Hawke, B. R. (2000). Imaging of lunar surface maturity. Journal of Geophysical Research E: Planets, 105(E8), pp. 20377–20386.

Lucey, P. G., Taylor, G. J., & Hawke, B. R. (1998). Global imaging of maturity: Results from Clementine and lunar sample studies. Lunar Planetary Science XXIX, abstract no. 1356.

McCraig, M. A., Osinski, G. R., Cloutis, E. A., Flemming, R. L., Izawa, M. R. M., Reddy, V., Applin, D. M. (2017). Fitting the curve in Excel®: Systematic curve fitting of laboratory and remotely sensed planetary spectra. Computers and Geosciences, 100(September 2016), pp. 103–114.

Moriarty, D. P., & Pieters, C. M. (2016). Complexities in pyroxene compositions derived from absorption band centers: Examples from Apollo samples, HED meteorites, synthetic pure pyroxenes, and remote sensing data. Meteoritics and Planetary Science, 51(2), pp. 207–234.

Mustard, J. F., Pieters, C. M., Isaacson, P. J., Head, J. W., Besse, S., Clark, R. N., … Tompkins, S. (2011). Compositional diversity and geologic insights of the Aristarchus crater from Moon Mineralogy Mapper data. Journal of Geophysical Research E: Planets, 116(5), pp. 1–17.

NASA. (2020). NASA's Lunar Exploration Program Overview. Retrieved October 1, 2020, from https://www.nasa.gov/sites/default/files/atoms/files/artemis_plan-20200921.pdf.

Nettles, J. W., Besse, S., Boardman, J., Combe, J.-P., Clark, R., Dhingra, D.,. (2010). Progress toward a new lunar optical maturity measure based on Moon Mineralogy Mapper (M3) data. LPI, (1533),pp. 2217.

Nettles, J. W., Staid, M., Besse, S., Boardman, J., Clark, R. N., Dhingra, D.,Taylor, L. A. (2011). Optical maturity variation in lunar spectra as measured by Moon Mineralogy Mapper data. Journal of Geophysical Research E: Planets, 116(7), pp. 1-20.

Pieters, Carlé M., Klima, R. L., & Green, R. O. (2019). Compositional Analysis of the Moon in the Visible and Near-Infrared Regions. Remote Compositional Analysis, pp. 368–392.

Pieters, Carle M, Boardman, J., Buratti, B., Chatterjee, A., Clark, R., Glavich, T.,(2009). The Moon Mineralogy Mapper (M3) on Chandrayaan-1. Current Science, pp. 500–505.

Press, W. H., & Teukolsky, S. A. (1990). Savitzky-Golay Smoothing Filters. Computers in Physics, 4(6), pp. 669.

Savitzky, A., & Golay, M. J. E. (1964). Smoothing and Differentiation of Data by Simplified Least Squares Procedures. Analytical Chemistry, 36, pp. 1627–1639.

Singer, R. B., & Roush, T. L. (1985). Effects of temperature on remotely sensed mineral absorption features. Journal of Geophysical Research: Solid Earth, 90(B14), pp. 12434–12444.

Taylor, L. A., Pieters, C. M. C. M., Keller, L. P., Morris, R. V., Mckay, D. S., Taylor, A., Mckay, D. S. (2001). Lunar Mare Soils: Space weathering and the major effects of surface-correlated nanophase Fe. Journal of Geophysical Research, 106(E11),pp. 27985–27999.